Investigation of the relationship between optical auroral forms and HF radar E region backscatter

S. E. Milan, M. Lester, N. Sato, H. Takizawa, J.-P. Villain

Ann. Geophysicae 18, 608–617 (2000) © EGS – Springer-Verlag 2000

Annales Geophysicae

Investigation of the relationship between optical auroral forms and HF radar E region backscatter

S. E. Milan[1], **M. Lester**[1], **N. Sato**[2], **H. Takizawa**[3], **J.-P. Villain**[4]

[1] Department of Physics and Astronomy, Leicester University, Leicester LE1 7RH, UK
[2] National Institute of Polar Research, Tokyo 173, Japan
[3] Tohoku University, Sendai 980-8578, Japan
[4] Centre National de la Recherche Scientifique, Orléans, France

Received: 19 August 1999 / Revised: 3 March 2000 / Accepted: 7 March 2000

Abstract. The SuperDARN HF radars have been employed in the past to investigate the spectral characteristics of coherent backscatter from *L*-shell aligned features in the auroral E region. The present study employs all-sky camera observations of the aurora from Husafell, Iceland, and the two SuperDARN radars located on Iceland, Þykkvibær and Stokkseyri, to determine the optical signature of such backscatter features. It is shown that, especially during quiet geomagnetic conditions, the backscatter region is closely associated with east-west aligned diffuse auroral features, and that the two move in tandem with each other. This association between optical and radar aurora has repercussions for the instability mechanisms responsible for generating the E region irregularities from which radars scatter. This is discussed and compared with previous studies investigating the relationship between optical and VHF radar aurora. In addition, although it is known that E region backscatter is commonly observed by SuperDARN radars, the present study demonstrates for the first time that multiple radars can observe the same feature to extend over at least 3 h of magnetic local time, allowing precipitation features to be mapped over large portions of the auroral zone.

Key words: Ionosphere (particle precipitation; plasma waves and instabilities)

Introduction

Several studies, including those of Villain *et al.* (1987, 1990), Hanuise *et al.* (1991) and Milan and Lester (1998, 1999), have employed HF radars, such as those which form SuperDARN (Greenwald *et al.*, 1995), to investigate the spectral characteristics of coherent backscatter from decametre-wavelength E region irregularities in the auroral electrojet region. In these studies, the E region backscatter generally takes the form of *L*-shell aligned features 2°–3° of latitude in width, within the near-range portion of the radar field-of-view. The dominant direction of irregularity drift within this backscatter region is eastward or westward if the observations are made in the westward or eastward electrojet regions, respectively. The present study demonstrates that during two intervals of simultaneous observation of such E region features within the fields-of-view of two SuperDARN radars, concurrent all-sky camera optical measurements show these to be closely associated with diffuse visible aurora. Such observations have repercussions for the irregularity generating mechanisms within these regions, and this is discussed with reference to similar work conducted during the early 1970s with VHF radars.

Experimental arrangement

The radar measurements from the present study were made by the two SuperDARN radars situated on Iceland: the Iceland East and Iceland West radars located at Þykkvibær (63.77°N, 339.46°E) and Stokkseyri (63.86°N, 337.98°E), respectively. These radars sound along sixteen beams, separated by 3.24° in azimuth, with the boresite of each radar being 30° east of north and 59° west of north in the case of the Iceland East and West radars, respectively. Each beam is gated into 75 range bins. Observations from two intervals will be presented, during which the radars operated in slightly different modes. During the first interval (study I), 0300 to 0504 UT, 29 September, 1998, the Þykkvibær radar had a range to the first gate of 180 km, and a gate length of 45 km; in the case of the Stokkseyri radar, these were 540 km and 30 km, respectively. Figure 1 indicates the locations of the fields-of-view of the two radars, though only the first 25 range gates of each are

Correspondence to: S. E. Milan
e-mail: Steve.Milan@ion.le.ac.uk

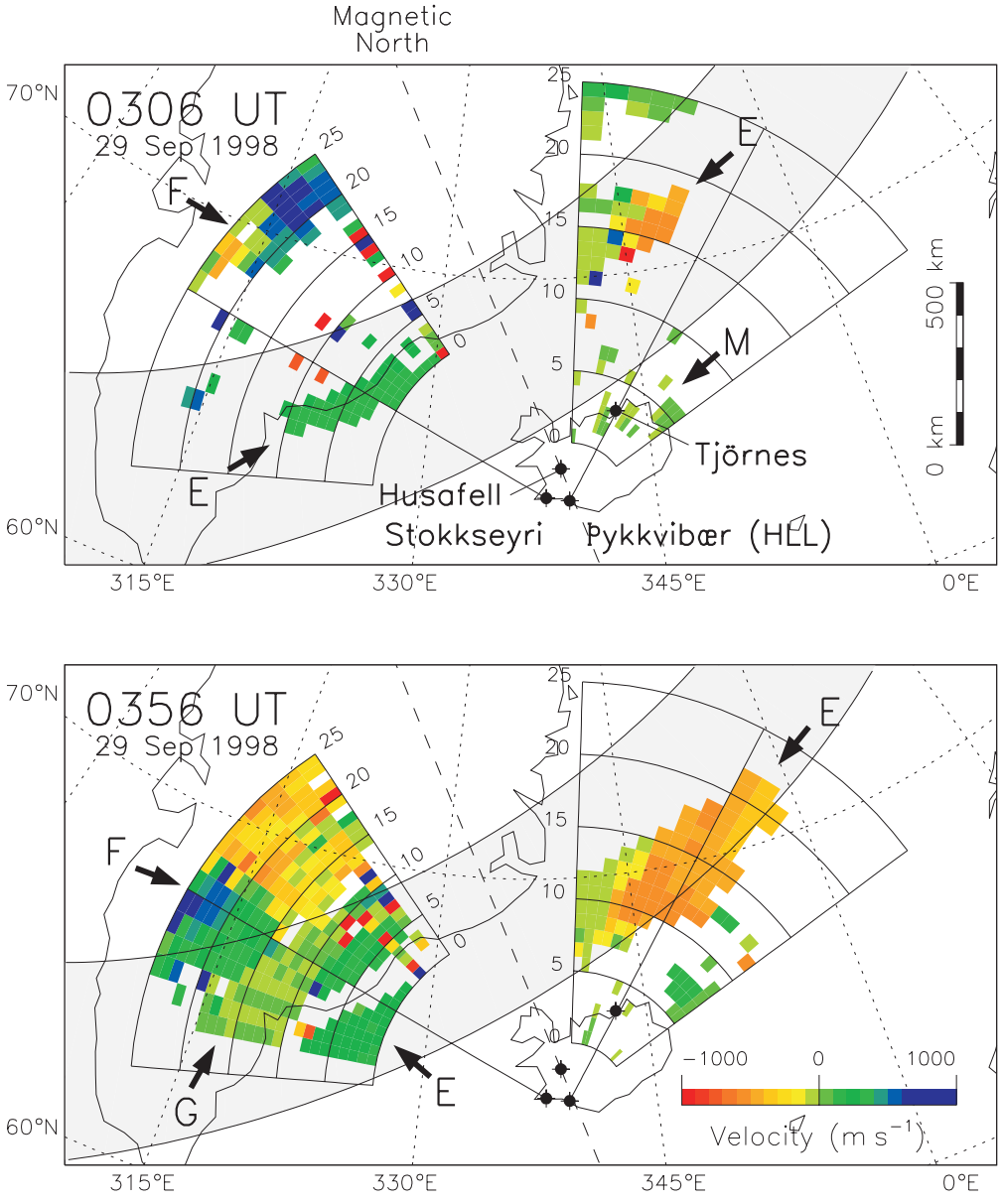

Fig. 1. A map indicating the locations of the Þykkvibær and Stokkseyri SuperDARN radars and the Husafell all-sky camera site employed in the present study. The location of the all-sky camera site at Tjörnes, to be employed in a future campaign, is also indicated. The SAMNET station Hella (*HLL*) is co-located with the Þykkvibær radar. The locations of the first *25 range gates* of the radars's fields-of-view for study interval I are shown, as well as the statistical location of the auroral oval for quiet geomagnetic conditions. Line-of-sight Doppler velocity determined for the radar scans starting at 0306 and 0356 UT during study interval I are *colour-coded*. Letters *E*, *F*, *G*, and *M* identify E region, F region, ground, and meteor backscatter, respectively

shown as only near-range scatter is of interest to this study. Included in this figure is the location of the statistical auroral oval (Feldstein and Starkov, 1967) for low geomagnetic activity levels, indicating that the oval crosses the near-range fields-of-view of both radars during this interval. The Stokkseyri radar was operating at a frequency of 11.5 MHz and the Þykkvibær radar was scanning in frequency between 10 MHz and 17 MHz in approximately 1 MHz steps, completing a frequency sweep every 14 min.

During the second interval (study II), 2200 UT, 15 February, 1999 to 0200 UT on the following day, both radars operated with a range to the first gate of 180 km and a gate length of 15 km, and both at a frequency near 11 MHz. The range resolution was hence much improved during this second study period: the extent of the whole field-of-view (all 75 range gates) of the two radars is the same as that indicated for only the first 25 range gates of the Þykkvibær radar in Fig. 1.

The all-sky camera (ASC) employed in the study was located at Husafell (64.67°N, 338.97°E), Iceland (see Fig. 1). The method of observation has been described in detail by Sato and Saemundson (1987). Figure 2 illustrates the mapping of the radar fields-of-view during study period I into the northern portion of the ASC field-of-view. The ASC was aligned with respect to the magnetic meridian (indicated in Fig. 1), with east to the left and west to the right of each ASC image. The horizon describes a circle around the periphery of each image, at an angle of 90° from the zenith; the point directly overhead the ASC, a zenith angle of 0°, is located at the centre of the field-of-view. A fundamental limitation of ground-based observations of the aurora is the ambiguity in determining the location of an optical feature without a detailed knowledge of the altitude profile of the emission intensity. Only auroral features situated directly overhead the observing site can be located with certainty,

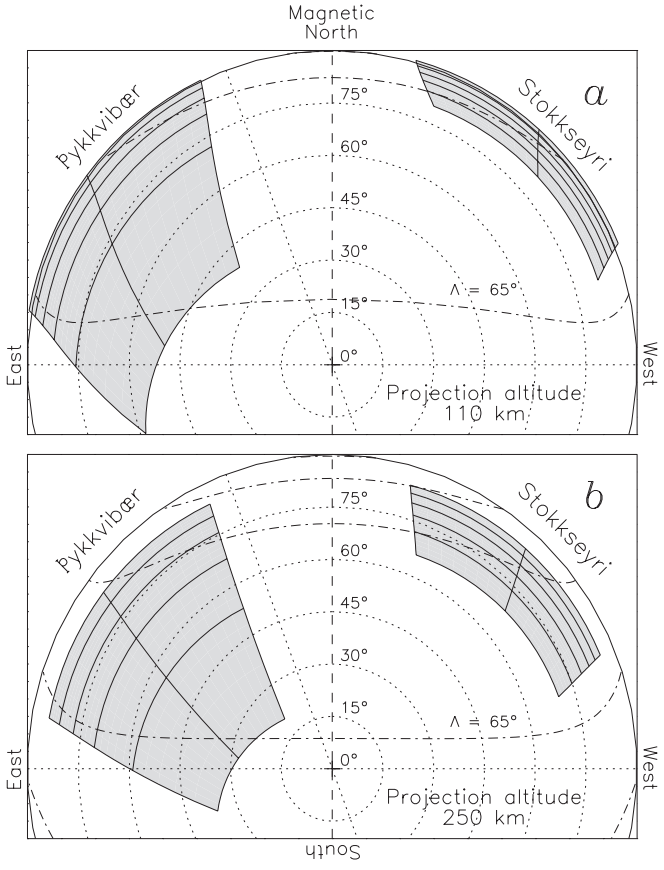

Fig. 2a, b. The mapping of the near-range Þykkvibær and Stokkseyri fields-of-view during study interval I into the field-of-view of the Husafell all-sky camera for two assumed auroral emission altitudes, **a** 110 km and **b** 250 km

the error in the mapping increasing with increasing zenith angle. Most aurora produce emission over a range of altitudes, and hence even narrow features located at a given geographic location appear spread in zenith angle within an ASC field-of-view. This will be discussed further later in relation to actual observations. In terms of mapping the location of optical features within the radars' fields-of-view, a single emission altitude for the aurora must be assumed. Figure 2a, b indicates the locations of the first 25 range gates of the two radars (for study interval I), for assumed auroral emission altitudes of 110 km (E region) and 250 km (F region), respectively. Dot-dashed lines indicate the loci of magnetic latitudes $\Lambda = 60°$, 65°, 70°, and 75°. In general, increasing the assumed emission altitude decreases the zenith angles to which the radars' fields-of-view map.

Observations

Study interval I

During the first study interval, 0300 to 0504 UT, 29 September, 1998, the instrumentation on Iceland was located within the region of the westward auroral electrojet (magnetic local time MLT ≈ UT). Figure 1 illustrates the radar measurements of line-of-sight Doppler velocity from two times during this interval, 0306 and 0356 UT. Positive and negative velocities represent irregularity drift toward and away from each radar, respectively. Several regions of backscatter are observed, the type of backscatter being denoted by letters in the figure. The altitude from which the backscatter originates can be determined using interferometric techniques in the manner outlined in Milan *et al.* (1997) and Milan and Lester (1999). It is found that those regions denoted "F" are backscatter from the F region ionosphere, and are not of interest to the present study. "G" indicates a region of ground backscatter, which tends to have very low Doppler velocity and spectral width. At the nearest ranges, backscatter from the ionization trails of meteoroids is observed (Hall *et al.*, 1997), this meteor scatter appearing as the sporadic echoes denoted "M". The backscatter of interest to this study originates at E region altitudes and tends to take the form of *L*-shell- or auroral oval-aligned features, denoted "E". Similar features have previously been discussed by Villain *et al.* (1987, 1990) and Milan and Lester (1998), though it has not been demonstrated previously that these features can be observed simultaneously by two radars over, in this case, 3 h of MLT in zonal extent. In the Þykkvibær and Stokkseyri radar fields-of-view the velocities associated with these features are negative and positive, respectively. This is consistent with eastward drift, as expected in the westward electrojet region. Between 0306 and 0356 UT, the E region scatter progresses slowly equatorward. This is shown more clearly in Fig. 3a, b which are range-time-power plots of radar backscatter from beam 5 of both the Þykkvibær and Stokkseyri radars. The E region backscatter features of interest appear between range gates 1 and 22 of the Þykkvibær observations (Fig. 3a) and gates 0 and 15 of the Stokkseyri observations (Fig. 3b). Prior to approximately 0420 UT, an equatorward motion of the radar backscatter is observed, in the case of the Stokkseyri radar to the very nearest ranges of the field-of-view (remembering that the range to the first gate and the gate length is different for the two radars). After 0420 UT, the backscatter region returns poleward, which in the case of the Þykkvibær observations, accompanies a bifurcation of the backscatter region.

The optical observations from this interval will now be described. A keyogram of the ASC observations is presented in Fig. 3c. This indicates the time-variation of the auroral emission intensity, as a function of zenith angle, along the magnetic meridian of the ASC field-of-view. A greyscale is employed to represent observed intensity, more intense features appearing darker. In addition, in Fig. 4b, d, f, h, j and l all-sky images are illustrated from selected times during this interval, as indicated by arrows at the top of Fig. 3 (the first two also correspond to the times illustrated in Fig. 1). Note that the optical intensity is marked in arbitrary units and the scale employed differs from image to image in Fig. 4 to emphasis the features under discussion. Bright

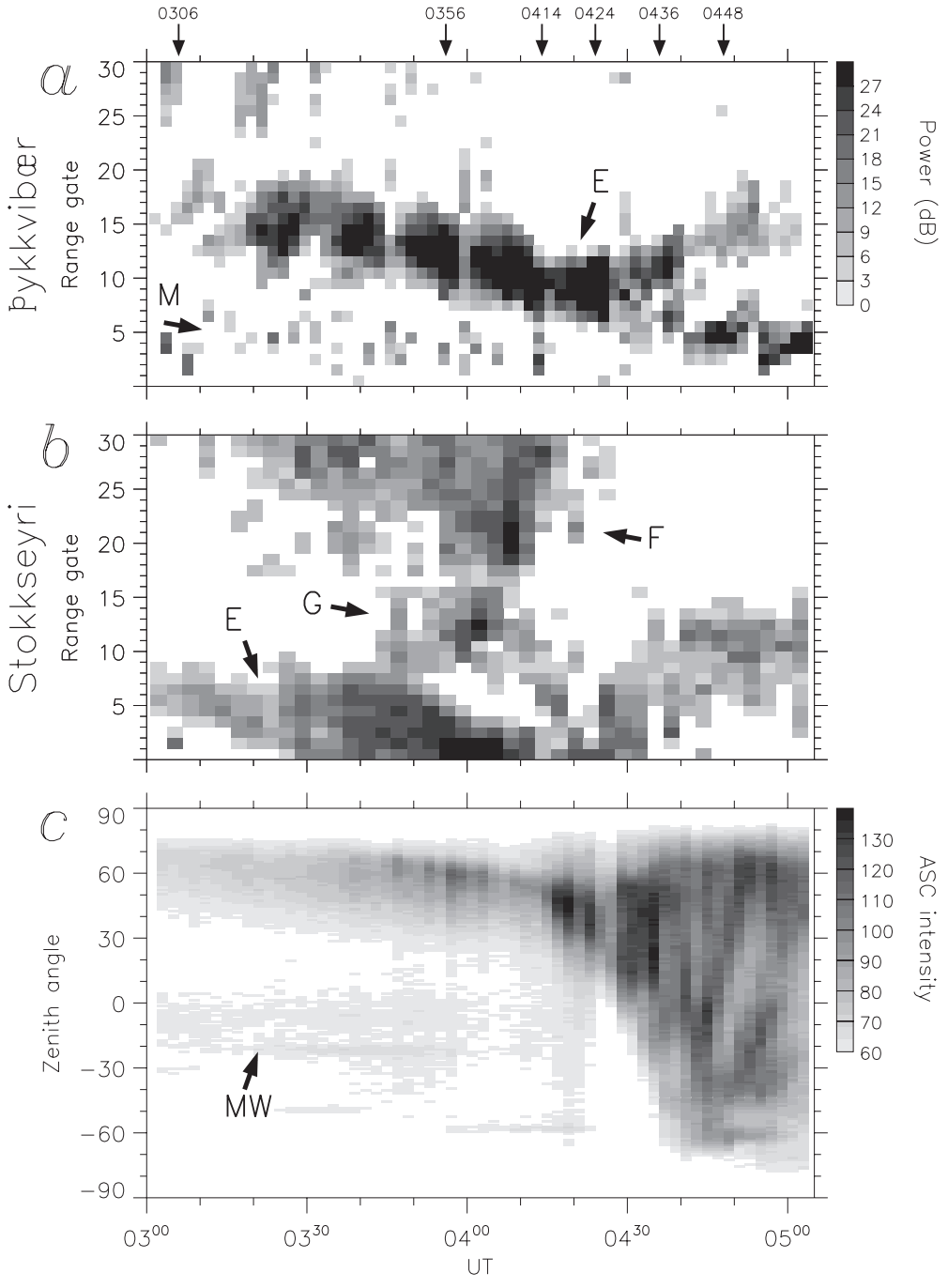

Fig. 3. a, **b** Range-time-power plots of the near-range portion of beam 5 of the Þykkvibær and Stokkseyri radars, during study interval I. *Letters* have the same meaning as in Fig. 1. **c** A keyogram of the auroral emission intensity observed by the Husafell all-sky camera, as a function of zenith angle along the magnetic meridian. *MW* identifies the Milky Way in the optical observations. *Arrows* at the top indicate times at which snapshots of the aurora are shown in Fig. 4

points within the images are stars or planets, Fig. 4b indicates the locations of α Auriga and α Lyra, and Fig. 4f that of Jupiter, which are employed to verify the orientation of the camera. Also present is a faint band of luminosity which runs from geographic east to west (magnetic NW to SE) which corresponds to the Milky Way (indicated "MW" in Fig. 4b and Fig. 3c). At the start of the interval, the ASC observations consist of a faint magnetic east-west aligned arc to the north of Iceland, at a zenith angle of 70°, which gains in intensity and gradually drifts southward to a zenith angle of 55° by 0415 UT. After 0415 UT this arc intensifies considerably and splits into two main features, the most poleward of which drifts poleward to 70° and the most equatorward of which expands rapidly equatorward, over the zenith of the ASC and into the southern portion of the field-of-view, to −65°. During this interval, significant structure is observed between the northern and southern extremes of the auroral emission.

As mentioned previously, auroral emission can be observed from a broad range of altitudes. This is best demonstrated in Fig. 4d and f. At these times the arc feature observed appears to have a well-defined "poleward" boundary, but a more gradual decrease in intensity at its "equatorward" boundary. In fact, the arc feature is probably narrower in latitude than at first appears, with the "poleward" boundary representing the lower edge of the arc and the diffuse "equatorward"

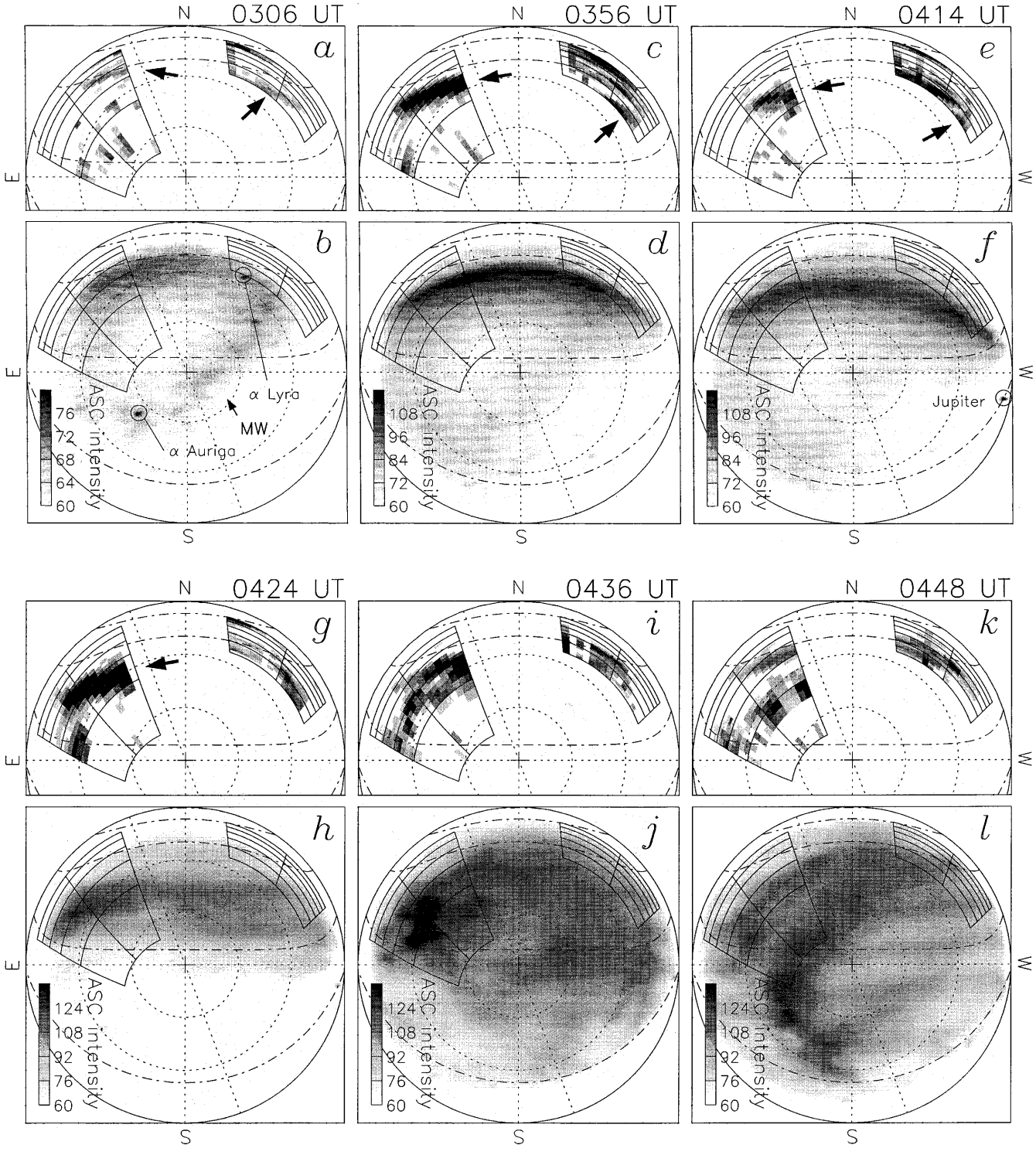

Fig. 4a–l. The *upper panels* show the radar backscatter projected into the all-sky camera field-of-view from the six times indicated by *arrows* in Fig. 3. The *lower panels* show simultaneous all-sky camera images. *Arrows* in the *upper panels* indicate the regions of backscatter which should be compared with features in the all-sky camera images. *MW* identifies the Milky Way in the optical observations

boundary represents the fall-off of emission intensity with increasing altitude.

Figure 3 does not allow a direct comparison of the radar observations in Fig. 3a, b with the ASC observations of Fig. 3c as the range scales are different for each instrument (remembering again that the range to the first gate and the gate length is different for the two radars), but does indicate similar trends in the motions of the E region backscatter region (radar aurora) and the optical aurora. That is: an equatorward drift of a band of aurora prior to 0415 UT and thereafter expansion both poleward and equatorward. Inspection of magnetograms from high-latitude stations of the IMAGE (Viljanen and Häkkinen, 1997) and SAMNET

(Yeoman *et al.*, 1990) magnetometer networks indicates that the onset of a substorm expansion phase occurred near 0410 UT. This is exemplified in Fig. 5 which presents H-, D-, and Z-component magnetograms from the Hella (HLL) SAMNET station, which is co-located with the Þykkvibær radar. Prior to approximately 0400 UT the magnetograms are quiet. The negative bay in the H component after this time is indicative of the presence of a substorm-associated westward electrojet. The negative excursion of the Z component indicates that the centre of this electrojet is located poleward of the magnetometer station. These observations suggest that the bifurcation and structure observed within the optical and radar aurora after 0415 UT corresponds to substorm break-up.

A direct comparison of the radar and optical observations is made in Fig. 4. For each ASC image, the simultaneous backscatter power observations from each radar are projected onto the field-of-view of the Husafell ASC (Fig. 4a, c, e, g, i and k). The backscatter power is represented by the same greyscale employed in Fig. 3. Those regions of backscatter which originate in the E region and which should be compared with the optical aurora are indicated by arrows in Fig. 4a, c, e and g. A very close correspondence between radar and optical aurora exists at these times. A projection altitude of 250 km has been employed as this appears to give the best co-location of the radar and optical observations in this case; this will be discussed in more detail later. After approximately 0430 UT (Fig. 4i and k) the Þykkvibær radar backscatter region bifurcates and the low latitude portion of the backscatter progresses equatorward. This is mirrored in the optical observations (see especially Fig. 4l), but the correspondence between optical and radar features is no longer as clear as previously.

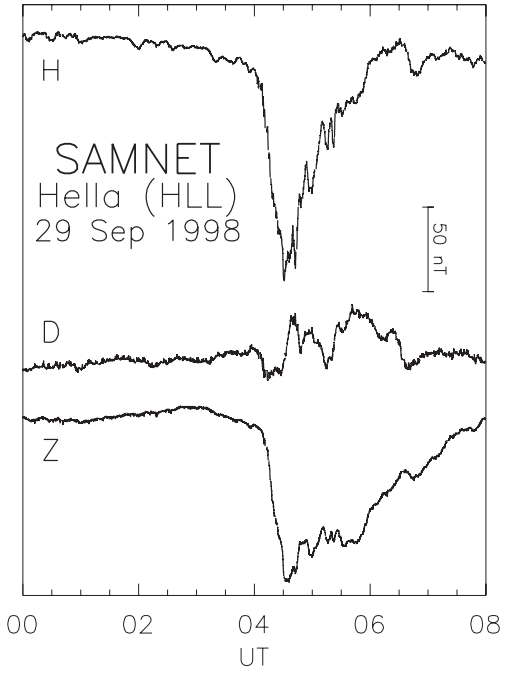

Fig. 5. The *H*-, *D*-, and *Z*-component magnetograms from study interval I, as measured by the HLL SAMNET station co-located with the Þykkvibær radar, indicating the occurrence of the magnetic signature of a substorm after 0410 UT

Study interval II

During the second interval of study, radar measurements were made between 2200 UT, 15 February, and 0200 UT, 16 February, 1999. Unfortunately, the clouds above Husafell parted for only the brief period between 2353 UT and 0035 UT, and so ASC images are available from this interval only. However, even at times with no corresponding optical information, the radar observations are of interest. During this interval, the radar range resolution, at 15 km, is significantly improved over that in study interval I. Figure 6 presents maps of backscatter power and line-of-sight Doppler velocity from the Þykkvibær and Stokkseyri radars at six representative times from study interval II. Throughout this period multiple, parallel, *L*-shell-aligned backscatter features are observed. (As in study interval I, large regions of backscatter in the far field-of-view originate in the F region and are not of interest to the present study.) In general, those features in the near ranges which are of greatest backscatter power are observed in both radars' fields-of-view simultaneously, most obvious in Fig. 6e, g, where two parallel features are present. In some cases, up to four parallel features can be observed in the field-of-view of at least one radar, as indicated by arrows in Fig. 6c. On occasion these *L*-shell-aligned backscatter features can be observed to extend over three hours of local time, such as the most poleward feature in Fig. 6a. Individual features can be as narrow as 30 to 100 km, resolvable, presumably, because of the increased spatial resolution of the radar scans, but the overall E region backscatter region tends to be several degrees of latitude in width. The Doppler velocity of the backscatter is predominantly negative in Stokkseyri and positive in Þykkvibær, consistent with westward flow in the eastward electrojet. There are regions of backscatter, however, for instance the most poleward E region feature of the four indicated by arrows in Fig. 6c, in which the drift is in the opposite sense, suggesting the presence of a westward electrojet. Moreover, within the eastward electrojet, the velocity within two parallel features is not necessarily uniform, most clearly seen in Fig. 6d in the Þykkvibær backscatter, in which a higher- and lower-velocity channel exist.

After approximately 2350 UT (Figs. 6i–l) only a single backscatter feature is observed in the near-range of the fields-of-view. This period corresponds to the time when ASC images are available. At the start of this interval a very faint and somewhat diffuse auroral feature is observed near the northern extreme of the ASC field-of-view, which later drifts equatorward. Figure 7 presents two ASC images from 0000 UT and 0030 UT. Note that the contrast in these images has been stretched considerably to emphasise the auroral feature. The approximate location of the lower border of the arc is superimposed on each image, represented as a dot-dashed line. The mapped geographic location

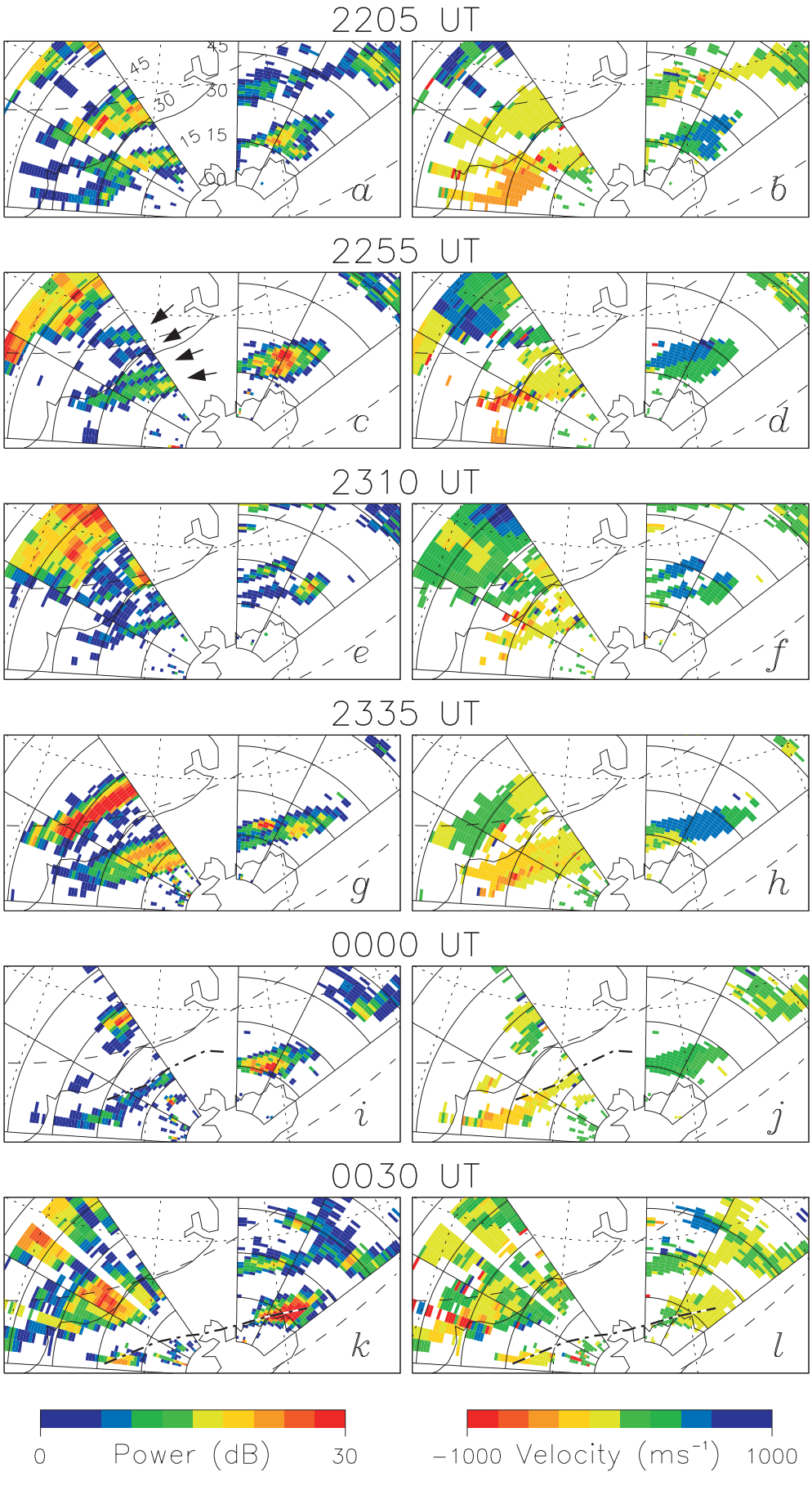

Fig. 6a–l. Backscatter power (*left panels*) and Doppler velocity (*right panels*) observed at six representative times during study interval II. *Dashed lines* indicate the poleward and equatorward edges of the statistical oval. The location of an equatorward-progressing optical arc observed between 2350 and 0035 UT is shown in **i** to **l** by a *dot-dashed line*

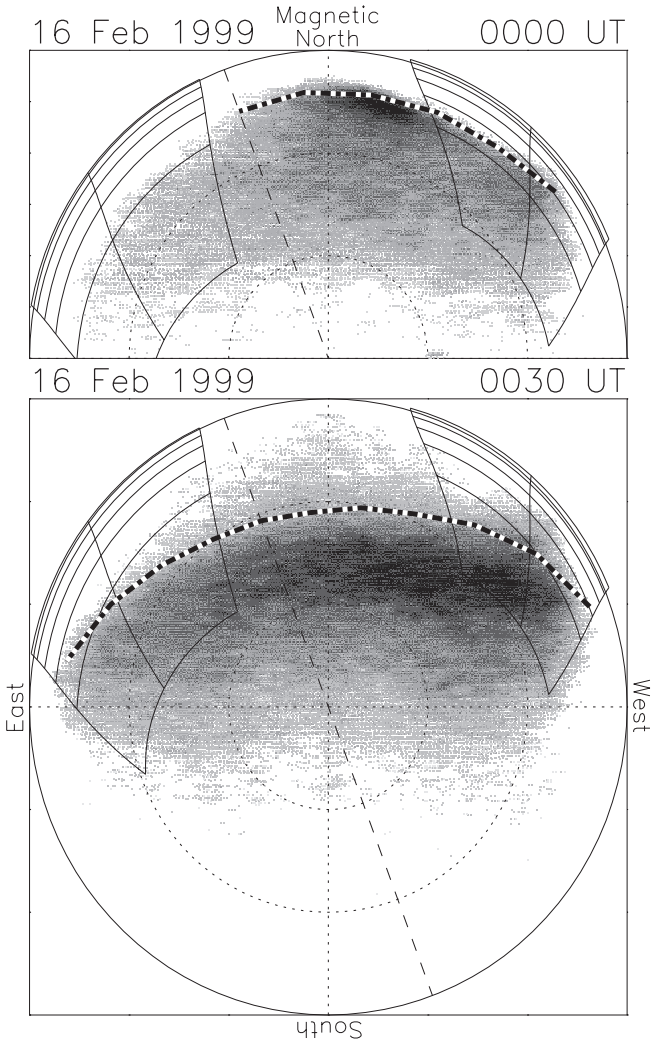

Fig. 7. The optical signature of the arc observed during study interval II

of this dot-dashed line, assuming an emission altitude of 110 km, has been indicated in Figs. 6i–l. A good correspondence between the location of the auroral form and the equatorward-drifting backscatter feature is found.

Discussion and conclusions

Two intervals of simultaneous observation of optical and HF radar aurora, one each in the vicinity of the westward and eastward auroral electrojet, have been investigated. The first half of study interval I, prior to 0415 UT, was geomagnetically quiet. During this period a single, approximately *L*-shell-aligned optical arc was observed in the northern portion of the all-sky camera field-of-view, drifting slowly equatorward. At this time an *L*-shell-aligned backscatter feature was observed within the fields-of-view of both HF radars, which appeared closely associated with the optical arc and moved in tandem with it. The onset of a substorm expansion phase at 0415 UT, with substorm break-up observed by the ASC, marked the beginning of an interval during which the correspondence between the radar and optical features became less clear, though similarities were still observed in the motions and general features of the radar and optical aurora. Substorm break-up is known to adversely affect the performance of HF radars in two ways (see Milan *et al.*, 1999, for a detailed discussion of both effects). In the first, enhancement of electron density in the E region, known as sporadic- or auroral-E, produces deviation of the radar beams and "blanketing" of the ionosphere above. In the second, enhancement of the D region produces attenuation of the radar signal. The latter effect can produce a loss of radar backscatter, though this does not appear to be a concern during the present observations. However, an increase in the amount of ground backscatter observed by the Stokkseyri radar toward the end of the interval suggests that sporadic-E is indeed affecting the radar propagation. Ground backscatter is not observed by the Þykkvibær radar, where the observations appear unaffected by sporadic-E. In this case the separation of the radar and optical aurora must be due to a change in the nature of the precipitation associated with the auroral feature or with the generating mechanism of the irregularities responsible for the radar backscatter. A change in precipitation energy, for instance, could affect the altitude of emission of the aurora.

The best correlation between the locations of radar and optical aurora occurred under the assumption that the auroral emission originated primarily at an altitude of 250 km during study interval I and 110 km in study interval II. That is not to say, however, that we believe the optical and radar aurora are exactly co-located: the only way to determine the exact correspondence between radar and optical aurora is to remove the altitude ambiguity associated with the auroral emission by making observations of radar backscatter directly overhead the ASC location, at the zenith of the ASC field-of-view. This would also allow the true latitudinal width of the auroral features to be determined. Unfortunately, the present experimental set-up does not allow such observations to be made in association with radar observations of E region backscatter. An ASC located in northeast Iceland, however, would be ideally situated, under the near-range field-of-view of the Þykkvibær radar, to make such a comparison possible. Indeed, such an optical campaign is planned for September 1999 at Tjörnes (see Fig. 1). Prior to such a definitive study, the present observations suggest only that the optical and E region HF radar aurora are closely related.

The co-location of optical and some *F region* HF radar aurora in the dayside auroral region has been demonstrated previously (Rodger *et al.*, 1995; Milan *et al.*, 1999b, c), and Milan *et al.* (1998) indicated that the auroral oval tends to be a discrete target for HF radars. These studies, and the present observations, suggest that magnetospheric precipitation, or the electrodynamics associated with precipitation regions, are a primary generation mechanism for ionospheric irregularities, the targets from which HF coherent radars scatter. Also, Milan *et al.* (1999a) demonstrated that HF radar back-

scatter spectra increased in power and could gain subsidiary spectral peaks in the vicinity of auroral arcs, as identified by incoherent scatter techniques. The precipitation features discussed by Milan *et al.* (1999a) appeared small in comparison to the size of a radar range gate, and, in the absence of simultaneous optical data, were interpreted as discrete aurora. In the present case, the optical features identified with the radar backscatter appear more diffuse in nature, and the backscatter region associated with them can be several range gates in latitudinal extent, especially during study interval I; indeed the width of the backscatter region as a whole is close to the expected width of the auroral electrojets. This is similar to early work which demonstrated a relationship between VHF radar backscatter from metre-scale E region irregularities and the auroral electrojets (e.g. Greenwald *et al.*, 1973) and optical aurora (e.g. Balsley *et al.*, 1973; Greenwald *et al.*, 1975; Romick *et al.*, 1974; Hunsucker *et al.*, 1975). These studies suggested that while a relationship did exist, the radar and discrete optical aurora were located adjacent to each other, but were not co-located. In general, radar backscatter was observed equatorward of auroral luminosity features in the eastward electrojet region, and it was assumed that this relationship would be reversed in the westward electrojet. The implication was that the radar irregularities were generated in the horizontal Hall current that flowed adjacent to auroral arc features. Two slightly different interpretations of the observations were forwarded. In the first, this current flowed in a region of high electric field but low conductivity (relative to that produced by the precipitation within the arc) associated with the electrodynamics of the arc system (Greenwald *et al.*, 1973); the location of this high electric field region, poleward or equatorward of the arc, is thought to be opposite in the eastward and westward electrojets. The second interpretation invoked the electron density gradients at the edges of arcs: the northward- or southward-directed electric field of the eastward and westward electrojets favours the generation of irregularities by the gradient drift instability on the equatorward or poleward side of arcs (Balsley *et al.*, 1973). It should be noted that horizontal gradients should play a more influential rôle in the generation of irregularities in the HF regime than the VHF regime (e.g. St.-Maurice *et al.*, 1994). In the present study, we found the best co-location of radar and optical aurora if the emission altitude was assumed to be 250 and 110 km in study intervals I and II, respectively. If, however, a uniform altitude of, say, 200 km was employed, the radar backscatter would be located at the northern and southern edges of the optical aurora in the westward and eastward electrojet regions, respectively. In this case, the present observations would be consistent with the VHF radar studies.

In the context of HF radar observations of E region electrojet backscatter, our findings support the suggestion of Villain *et al.* (1987, 1990) that particle precipitation must be associated with these commonly observed radar features. Within E region scatter, Villain *et al.* (1987, 1990) identified HF radar backscatter spectra with characteristics consistent with the two-stream and electrostatic ion cyclotron instabilities, though in regions of sub-critical horizontal electric field, i.e. in regions in which the ion drift was below the threshold necessary for the generation of these instabilities. Their conclusion was that additional free energy could be available from vertically-moving electrons. More specifically, these were thought to be upward-moving thermal electrons carrying downward return current to close the upward current associated with electron precipitation. Again, this would be expected to occur adjacent to the luminosity feature, consistent with the present observation of aurora closely associated with the backscatter regions, though again suggesting that the two are not necessarily co-located. Further work is necessary: as reported by Villain *et al.* (1987, 1990) and also Milan and Lester (1998) and especially Milan and Lester (1999), a complex variety of spectral types and populations exist within HF radar backscatter from the auroral E region. The ultimate goal of the present line of investigation is to relate different spectral characteristics with features in the optical aurora. Unfortunately, the current data-set is insufficient to achieve this, and, as discussed already, an ASC located under the field-of-view of the Þykkvibær radar is needed to make such a detailed comparison possible.

In summary, this study indicates that during periods of low geomagnetic activity, *L*-shell-aligned features in HF radar backscatter from E region altitudes in the auroral electrojet regions have an optical counterpart and hence are associated with particle precipitation. A conclusive determination of the exact relationship between optical and radar aurora is made difficult by ambiguities in the altitude of emission of auroral forms. An experiment with a more favourable observational geometry is necessary to fully resolve this issue. However, the ability to image such electrojet scatter regions with many radars simultaneously potentially allows the SuperDARN network to map the location of precipitation features over large portions of the high latitude ionosphere.

Acknowledgements. CUTLASS is supported by the Particle Physics and Astronomy Research Council (PPARC grant PPA/R/R/1997/00256), UK, the Swedish Institute for Space Physics, Uppsala, and the Finnish Meteorological Institute, Helsinki. The optical auroral observation project in Iceland is supported by Grants in Aid for Overseas Science Survey (grant no. 07044104, 09044106) from the Ministry of Education, Science, Sports and Culture, Government of Japan (MONBUSHO) and by Dr. T. Saemundsson for the Science Institute, University of Iceland. The authors thank Dr I. R. Mann and Dr D. K. Milling for the SAMNET data. SAMNET is a PPARC National Facility deployed and operated by the University of York. SEM is supported on PPARC grant PPA/G/O/1997/000254.

The Editor in-chief thanks A.V. Kustov, G.C. Cerisier and another referee for their help in evaluating this paper.

References

Balsley, B. B., W. L. Ecklund, and R. A. Greenwald, VHF Doppler spectra of radar echoes associated with a visual auroral form: observations and implications, *J. Geophys. Res.*, **78,** 1681, 1973.

Feldstein, Y. I., and G. V. Starkov, Dynamics of auroral belt and polar geomagnetic disturbances, *Planet. Space Sci.*, **15,** 209, 1967.

Greenwald, R. A., W. L. Ecklund, and B. B. Balsley, Auroral currents, irregularities, and luminosity, *J. Geophys. Res.*, **78,** 8193, 1973.

Greenwald, R. A., W. L. Ecklund, and B. B. Balsley, Radar observations of auroral electrojet currents, *J. Geophys. Res.*, **80,** 3635, 1975.

Greenwald, R. A., K. B. Baker, J. R. Dudeney, M. Pinnock, T. B. Jones, E. C. Thomas, J.-P. Villain, J.-C. Cerisier, C. Senior, C. Hanuise, R. D. Hunsucker, G. Sofko, J. Koehler, E. Nielsen, R. Pellinen, A. D. M. Walker, N. Sato, and H. Yamagishi, DARN/SuperDARN: a global view of the dynamics of high-latitude convection, *Space Sci. Rev.*, **71,** 761, 1995.

Hall, G. E., J. W. MacDougall, D. R. Moorcroft, J.-P. St.-Maurice, A. H. Manson, and C. E. Meek, Super Dual Auroral Radar Network observations of meteor echoes, *J. Geophys. Res.*, **102,** 14 603, 1997.

Hanuise, C., J.-P. Villain, J.-C. Cerisier, C. Senior, J. M. Ruohoniemi, R. A. Greenwald, and K. B. Baker, Statistical study of high-latitude E-region Doppler spectra obtained with the SHERPA HF radar, *Ann. Geophysicae*, **9,** 273, 1991.

Hunsucker, R. D., G. J. Romick, W. L. Ecklund, R. A. Greenwald, B. B. Balsley, and R. T. Tsunoda, Structure and dynamics of ionization and auroral luminosity during the auroral events of March 16, 1972, near Chatanika, Alaska, *Radio Sci.*, **10,** 813, 1975.

Milan, S. E., and M. Lester, Simultaneous observations at different altitudes of ionospheric backscatter in the eastward electrojet, *Ann. Geophysicae*, **16,** 55, 1998.

Milan, S. E., and M. Lester, Spectral and flow angle characteristics of backscatter from decametre irregularities in the auroral electrojets, *Adv. Space Res.*, **23**(10), 1773, 1999.

Milan, S. E., T. B. Jones, T. R. Robinson, E. C. Thomas, and T. K. Yeoman, Interferometric evidence for the observation of ground backscatter originating behind the CUTLASS coherent HF radars, *Ann. Geophysicae*, **15,** 29, 1997.

Milan S. E., T. K. Yeoman, and M. Lester, The dayside auroral zone as a hard target for coherent HF radars, *Geophys. Res. Lett.*, **25,** 3717, 1998.

Milan, S. E., J. A. Davies, and M. Lester, Coherent HF radar backscatter characteristics associated with auroral forms identified by incoherent radar techniques: a comparison of CUTLASS and EISCAT observations, *J. Geophys. Res.*, **104,** 22 591, 1999a.

Milan, S. E., M. Lester, S. W. H. Cowley, J. Moen, P. E. Sandholt, and C. J. Owen, Meridian-scanning photometer, coherent HF radar, and magnetometer observations of the cusp: a case study, *Ann. Geophysicae*, **17**, 159, 1999b.

Milan, S. E., T. K. Yeoman, M. Lester, J. Moen, and P. E. Sandholt, Post-noon two-minute period pulsating aurora and their relationship to the dayside convection pattern, *Ann. Geophysicae*, **17**, 877, 1999c.

Rodger, A. S., S. B. Mende, T. J. Rosenberg, and K. B. Baker, Simultaneous optical and HF radar observations of the ionospheric cusp, *Geophys. Res. Lett.*, **22,** 2045, 1995.

Romick, G. J., W. L. Ecklund, R. A. Greenwald, B. B. Balsley, and W. L. Imhof, The interrelationship between the >130 keV electron trapping boundary, the VHF radar backscatter, and the visual aurora, *J. Geophys. Res.*, **79**, 2439, 1974.

St.-Maurice, J.-P., P. Prikryl, D. W. Danskin, A. M. Hamza, G. J. Sofko, J. A. Koehler, A. Kustov, and J. Chen, On the origin of narrow non-ion-acoustic coherent radar spectra in the high-latitude E region, *J. Geophys. Res.*, **99,** 6447, 1994.

Sato, N., and T. Saemundsson, Conjugacy of electron auroras observed by all-sky cameras and scanning photometers, *Mem. Natl. Inst. Polar Res., Spec. Issue*, **48,** 58, 1987.

Viljanen, A., and L. Häkkinen, IMAGE magnetometer network, in *Satellite-ground based coordination sourcebook*, Eds. M. Lockwood, M. N. Wild and H. J. Opgenoorth, ESA publications **SP-1198**, 111, 1997.

Villain, J.-P., R. A. Greenwald, K. B. Baker, and J. M. Ruohoniemi, HF radar observations of E region plasma irregularities produced by oblique electron streaming, *J. Geophys. Res.*, **92,** 12 327, 1987.

Villain, J.-P., C. Hanuise, R. A. Greenwald, K. B. Baker, and J. M. Ruohoniemi, Obliquely propagating ion acoustic waves in the auroral E region: further evidence of irregularity production by field-aligned electron streaming, *J. Geophys. Res.*, **95,** 7833, 1990.

Yeoman, T. K., D. K. Milling, and D. Orr, Pi2 pulsation polarization patterns on the UK Sub-Auroral Magnetometer Network (SAMNET), *Planet. Space Sci.*, **38,** 589, 1990.